12.6 THE LIMIT OF PREDICTABILITY IN THE STRATOSPHERE VERSUS TROPOSPHERE OF A COUPLED GCM

Cristiana Stan[1,*] and David M. Straus[1,2]
[1] Center for Ocean-Land-Atmosphere Studies, Calverton MD
[2]George Mason University, Fairfax VA

1. INTRODUCTION

The motivation for applying traditional forecast predictability tools to the stratospheric circulation in general and sudden warmings in particular arises from the presence of dramatic variability in the observed stratosphere, and the recent availability of very large forecast ensembles with a state-of-the-art forecast model that includes realistic representations of both troposphere and stratosphere.

2. MODEL DESCRIPTION

This model is the NCEP Climate Forecast System (CFS). The atmospheric GCM has a horizontal resolution of T62 of about 200 km with 64 sigma levels and the top at 0.2 hPa. Above 150 hPa there are 27 levels. The oceanic GCM is MOM3. The coupling between the atmosphere and ocean is realized through the interactive ensemble (Stan and Kirtman, 2007). In this coupling strategy the ocean model is coupled to the ensemble average of 6 atmospheric models that in turn are forced by the same SST. Each atmospheric model is initialized from slightly different initial condition, so that the 6 realizations of the atmosphere give a good sample of internal variability. The atmospheric initial conditions are taken from the NCEP/DOE AMIP R2 reanalyses, and are 6 hours apart. Thus, the atmospheric realizations can be interpreted as equally likely responses of the atmosphere to the same SST. For predictability studies, the atmospheric realizations in a single interactive ensemble represent outcomes of so called "identical twin experiments," with 15 pairs of twins available.

For each January in the 10-year period (1981-1990), 5 interactive ensemble forecasts (of length one year) were run from the same ocean initial condition representative of 1 January. Thus for each calendar year we have essentially 5 sets of identical twin experiments.

Corresponding author address: Cristiana Stan, COLA, Powder Mill Rd, Ste. 302, Calverton, MD, 20705-3106, e-mail: stan@cola.iges.org

3. SUDDEN STRATOSPHERIC WARMING

Charlton and Polvani (2007) in a recent paper have compiled a comprehensive list of all sudden stratospheric warming events in the last 50 years in the NCEP and ERA 40 data sets. Events occurring after 1970 are summarized in Table 1. We can see that during the analyzed period there are a few sudden stratospheric warming events that happen very close to the initialization time, so that the model should be able to capture them. We will not consider the events that happen during December, because they represent a forecast range of 12 months, beyond the expected predictability range of model skill.

Table 1 Sudden stratospheric warming events from Charlton and Polvani, 2007.

No.	Central date, NCEP-NCAR	Central date, ERA-40
11	2 Jan 1970	1 Jan 1970
12	17 Jan 1971	18 Jan 1971
13	20 Mar 1971	19 Mar 1971
14	2 Feb 1973	31 Jan 1973
15		9 Jan 1977
16	22 Feb 1979	22 Feb 1979
17	29 Feb 1980	29 Feb 1980
18		4 Mar 1981
19	4 Dec 1981	4 Dec 1981
20	24 Feb 1984	24 Feb 1984
21	2 Jan 1985	1 Jan 1985
22	23 Jan 1987	23 Jan 1987
23	8 Dec 1988	7 Dec 1988
24	14 Mar 1988	14 Mar 1988
25	22 Feb 1989	21 Feb 1989

In Figure 1, the left panels show the temperature (averaged over the Polar Cap north of 60^{o}N) at 10hPa for the stratospheric warming of 24 February 1984, 23 January 1987 and 22 February 1989 from the model and observations. The orange curves denote the 30 atmospheric realizations corresponding to the 5 interactive ensembles, the blue curve is the ensemble mean and the black curve corresponds to observations.

The zonal mean zonal wind at 10 hPa is plotted in the right panels for the same events using the same color coding. These three figures show that while some individual forecasts capture the strong easterlies, few if any capture the extent of the polar warming. The ensemble means clearly do not have any prediction skill for the sudden stratospheric warming events. Before we investigate why the model is not able to consistently forecast these events, it is useful to check if the model climatology agrees with the observed counterpart. We want to eliminate the possibilities that in the model the stratosphere is already too warm so it cannot get warmer, or that it is too cold and if it warms up, the temperature raise is not enough to catch up with the observations. Figure 2 shows the observed and modeled January and February climatology of zonal mean temperature. Figure 3 shows their difference. While the 10 hPa temperature bias in January is small poleward of 60°N, it does grow fairly substantially (over 8 degrees) in February. The zonal-mean zonal wind for observations and model are shown in Figure 4; it is clear that the model generally simulates the jet structure well, although the 10 hPa winds near the pole are somewhat weak in both months.

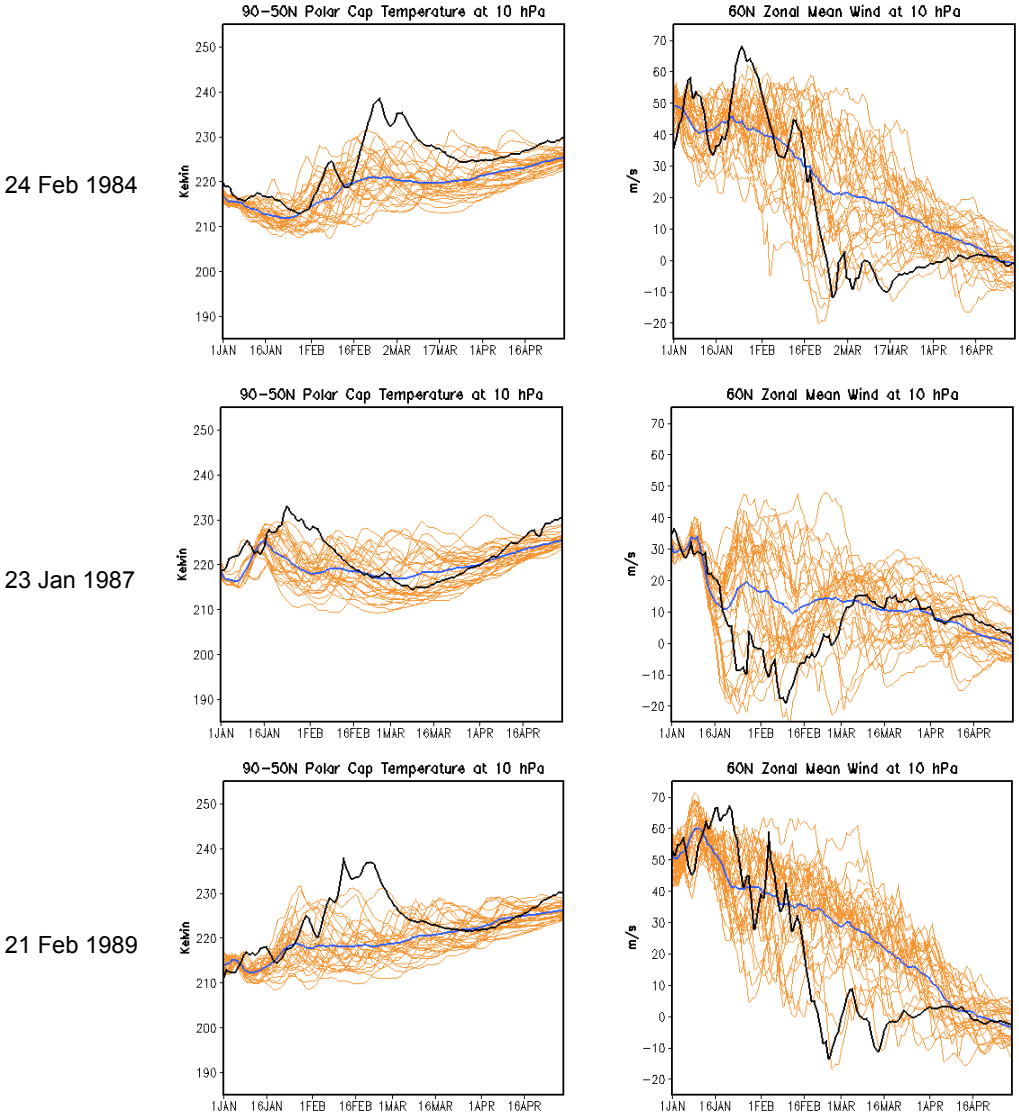

Figure 1 (left) Temperature (averaged over the Polar Cap north of 60°N) at 10hPa from the model and observations. (right) Zonal wind U (similarly averaged). The orange curves denote the 30 atmospheric realizations corresponding to the 5 interactive ensembles, the blue curve is the ensemble mean and the black curve corresponds to observations.

By now, it is well understood that stationary planetary waves, especially those involving zonal wavenumber 1 and 2, are essential for the occurrence of the sudden stratospheric events. Figure 5 shows the vertical distribution of the stationary waves in temperature for zonal wavenumber 1 and 2 in January. The amplitude and phase of both observations and model simulation are shown. The black solid line denotes the wave amplitude and the colored dashed line corresponds to the phase of the waves. (Blue is used for the negative phase, which is equivalent to eastward displacement of the ridge; red is used for the positive phase, equivalent to westward displacement). The amplitudes of both waves are realistic, if slightly too weak, in the model simulations. The phase simulation is quite realistic for zonal wavenumber 1, while there is some discrepancy between the model and observed phase for wavenumber 2.

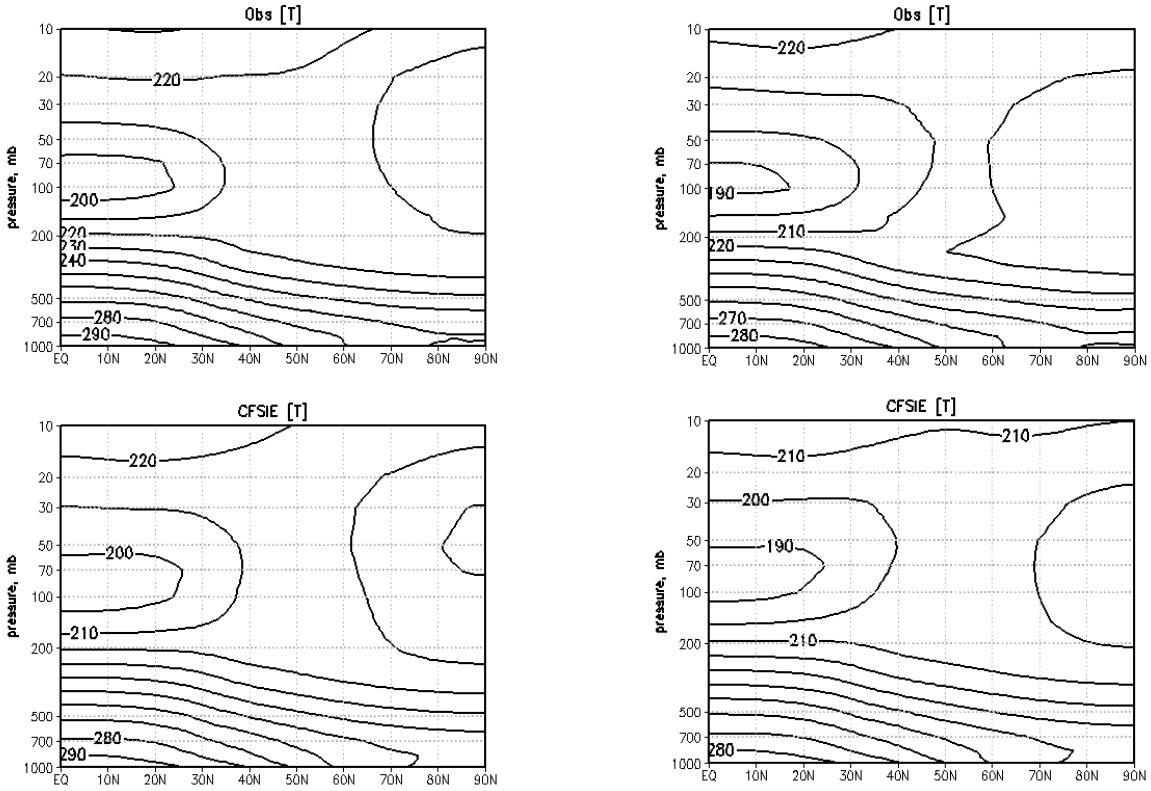

Figure 2 January (left) and February (right) climatology of the observed (top) and modeled (bottom) zonal mean temperature. Contour interval 10K.

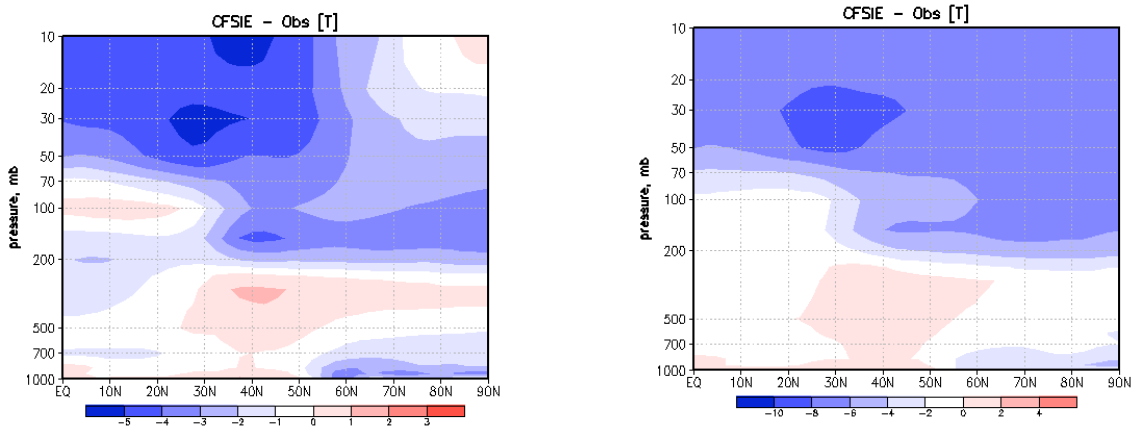

Figure 3 Model error of the zonal mean temperature simulation during January (left) and February (right).

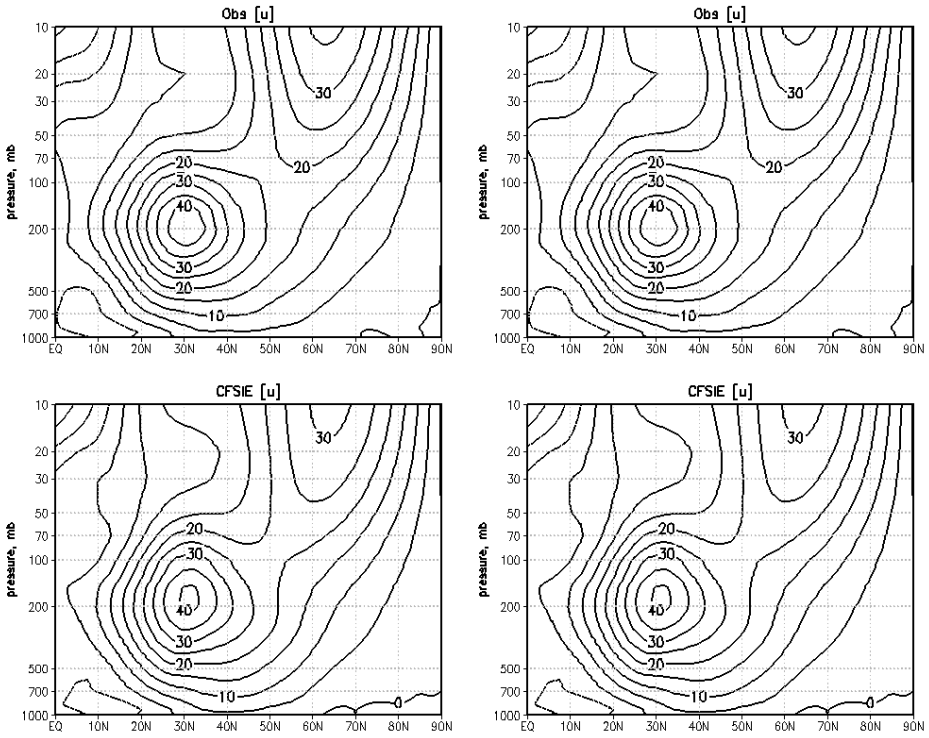

Figure 4 Meridional cross-section of the January (left) and February (right) zonal mean zonal wind climatology from observations (top) and model simulations (bottom).

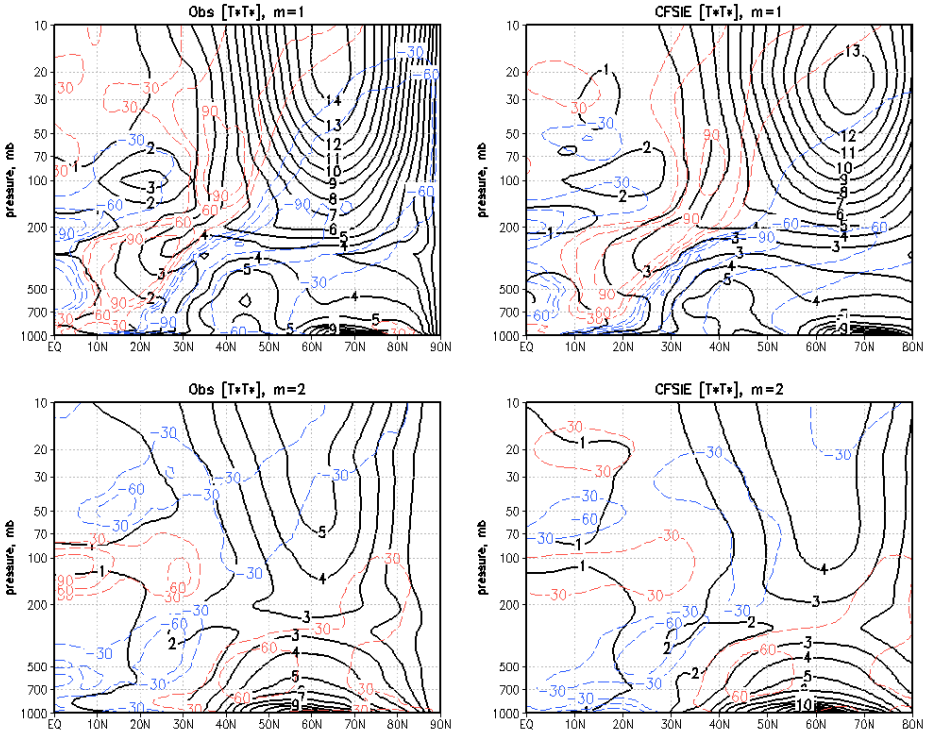

Figure 5 Meridional cross-section of amplitude (solid line) and phase (dashed line) for stationary wavenumber 1 (top) and 2 (bottom) from observations (left) and model simulations (right). Blue denotes negative phase and red positive phase.

Another quantity that can yield information about the wave propagation is the refraction index squared, shown in Figure 6. Here shading denotes regions of negative values, where the waves cannot propagate. Also contours greater than 100 were omitted, because very large values occurs in regions where the zonal wind equals the zonal phase velocity, i.e. near critical layers, where the waves break. In these regions, the index of refraction is not relevant. Meridional cross-sections of the refraction index for wavenumber 1 (upper panels) and wavenumber 2 (lower panels) during January indicate a similar structure in the model and the observations. This suggests that the wave activity in the model tends to behave realistically, since waves tend to propagate toward regions of large positive values of the index of refraction. Although the index of refraction in the high-latitude stratosphere is not quite as strong in the model as in the observations, the model has the right structure required to focus upward propagating wavenumber 1 and 2 activity into the high latitude stratosphere. A similarly good agreement is also found in the February climatology shown in Figure 7. The position of positive maxima is in the right place, and the regions of negative values, which are regions where by definition waves cannot enter, agree reasonably well. Since the index of refraction is a quantity very sensitive to the profile of the zonal mean zonal wind, a small change in the shape of the jet leads to a different configuration of the index, which means a different pattern in wave propagation. To quote M. McIntyre (1982) "…no matter what the troposphere is doing, conditions in the stratosphere have to be prepared in some special way before a major warming can take place…"

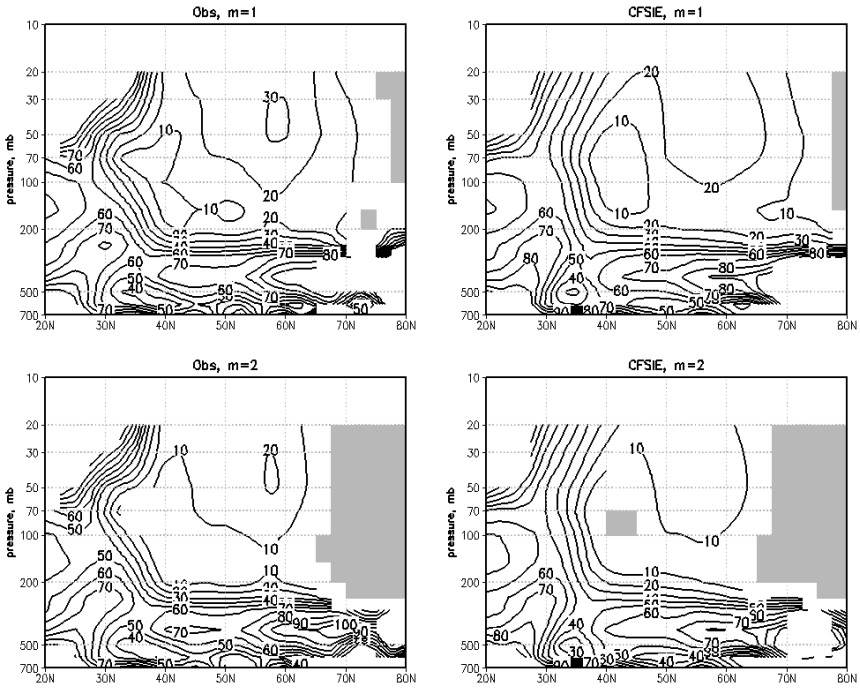

Figure 6 Meridional cross-section of the refractive index squared for the stationary zonal waves with wavenumber 1 (top) and 2 (low) from observations (left) and model simulations (right) in January. Regions with negative values are shaded. Contours with values greater than 100 are omitted.

4. PREDICTABILITY

These results suggest that a possible explanation for the model failure might be related to the intrinsic nature of stratospheric predictability. As mentioned earlier, the experimental design offers the perfect opportunity to look into the limit of predictability in the stratosphere versus troposphere. For each interactive ensemble, we have 15 identical twin pairs, for which the squared error of any quantity may be computed. Averaging the squared error over all pairs, then over all 5 ensembles, and finally over 10 years, yields a good estimate of error growth due solely to differences in the initial conditions. This error growth is driven by the degree of deterministic chaos that characterizes the dynamics of the region in which the prediction is made. Zonally averaging the mean

squared error allows for an expansion in terms of zonal wavenumbers.

Figure 8 shows the normalized forecast errors in the zonalwavenumber 1 field of zonal wind, meridional wind and temperature for three different levels: 850, 200 and 30 hPa. The saturation value (which provides the normalization) is calculated as the 10-day mean at the end of February. The squared errors are averaged between 50 and 70N. The black line denotes the total amplitude, which can be written as a sum of two terms, one giving the squared error due to the phase difference between the waves (shown in the green line) and the second giving the error due to the amplitude difference between the waves (shown in the yellow line). [A property of this decomposition is that the first term vanishes if the phases are equal, while the second term vanishes if the amplitudes are equal.]

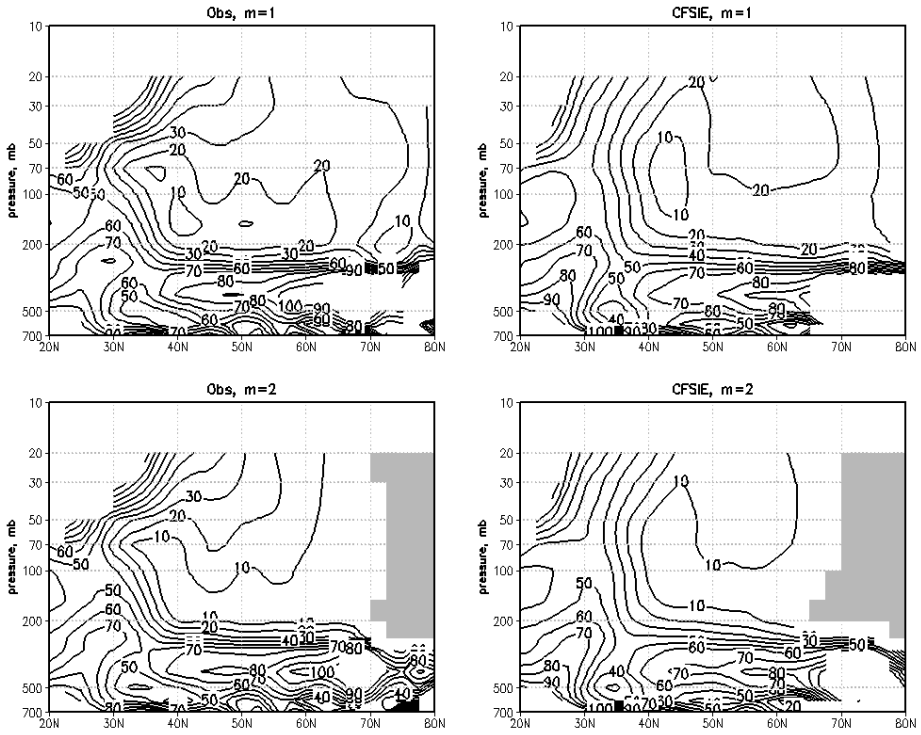

Figure 7 Same as Figure 6, but for February.

A first important result is that the magnitude of the (squared) error is dominated by the magnitude of the phase error. This suggests that the phase of the wave is an important factor in limiting the predictability. For wavenumber 1, the limit of predictability is comparable at all levels, about 20 days. For wavenumber 2 (shown in Figure 9), the limit of predictability appears to become smaller at higher levels. Another interesting, and likewise surprising result, is the shape of the error curve in temperature at 30 hPa. Rather than simply growing and saturating, the error decreases at large time, indicating a systematic decrease in variability towards the end of the winter season. To eliminate the suspicion that this behavior is an artifact of the model, we constructed the cross-sections of temperature variance (i.e. deviation from the ensemble mean), averaged over the same 50-70^{o}N latitudinal belt, for both wavenumbers 1 and 2, and compared them with the observations. These are shown in Figure 10. The systematic decrease in variability towards the end of boreal winter is indeed a natural feature of the stratosphere, and one that is not present in the troposphere.

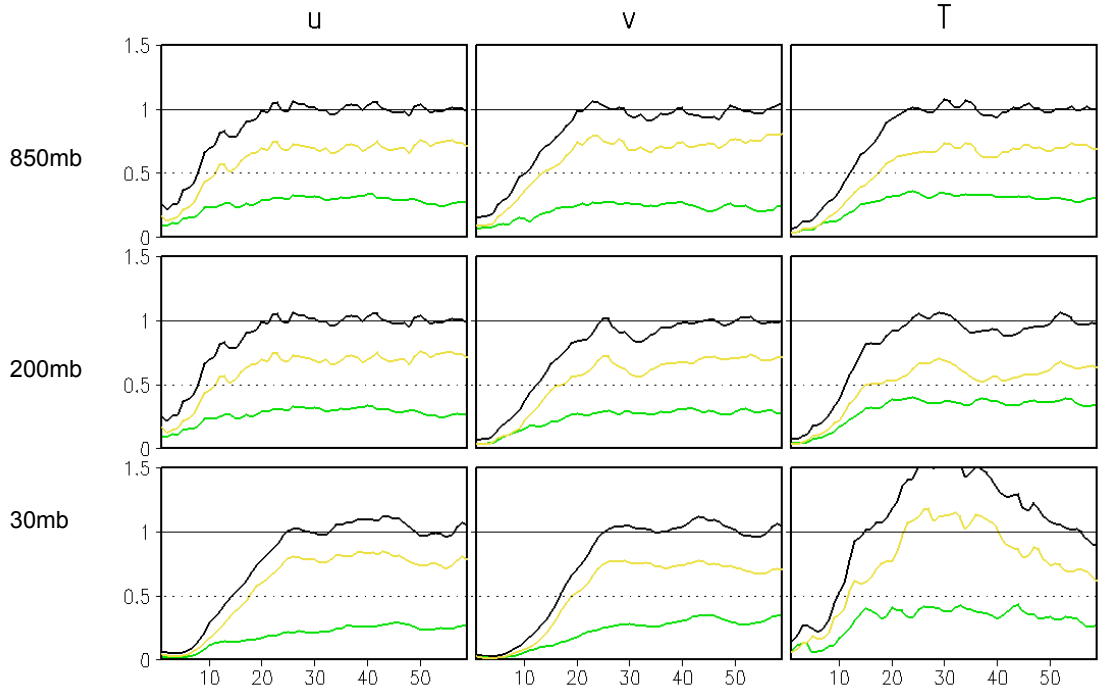

Figure 8 The normalized forecast errors in the zonal wavenumber 1 field of zonal wind, meridional wind and temperature for three different levels: 850, 200 and 30 hPa. The black line denotes the total amplitude, the green line represents the squared error due to the phase difference between the waves and the yellow line denotes the error due to the amplitude difference between the waves.

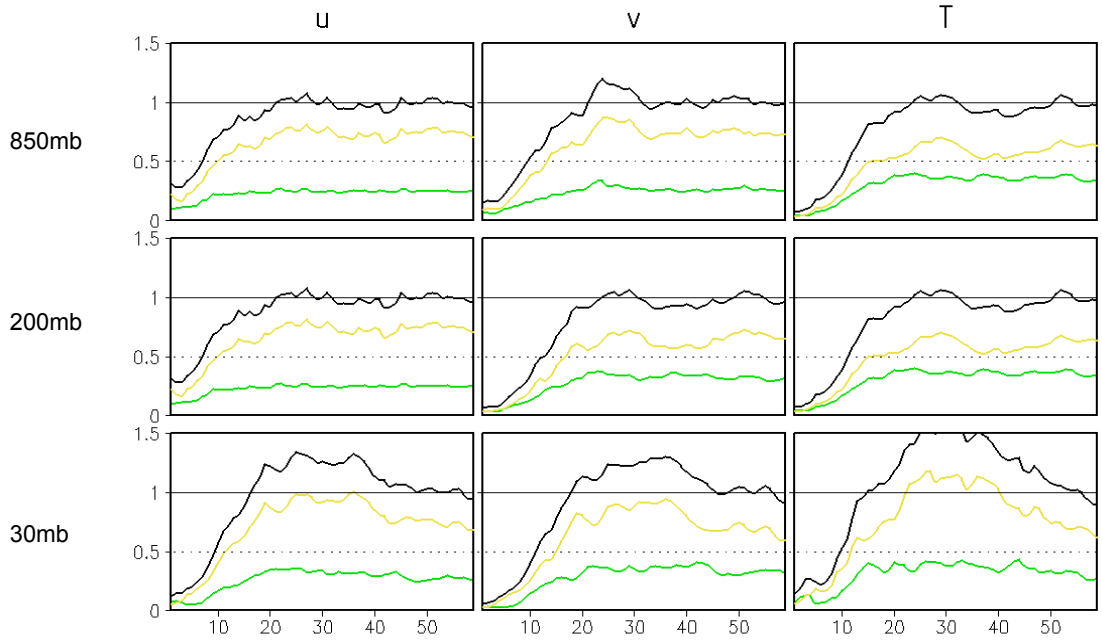

Figure 9 Same as Figure 8, but for zonal wavenumber 2.

As we know, sudden stratospheric warming events occur as a result of a special pattern in the wind and temperature fields. A good measure of the wave activity flux is the Eliassen-Palm (EP) flux and its divergence. Since the EP flux and its divergence are by definition zonally averaged quadratic quantities in the eddy fields, they can also be expressed as a sum over zonal wavenumbers. For each zonal wavenumber separately, we computed the squared error of EP flux divergence averaged over all 15 identical twin pairs in each ensemble, over each ensemble and over all 10 years.

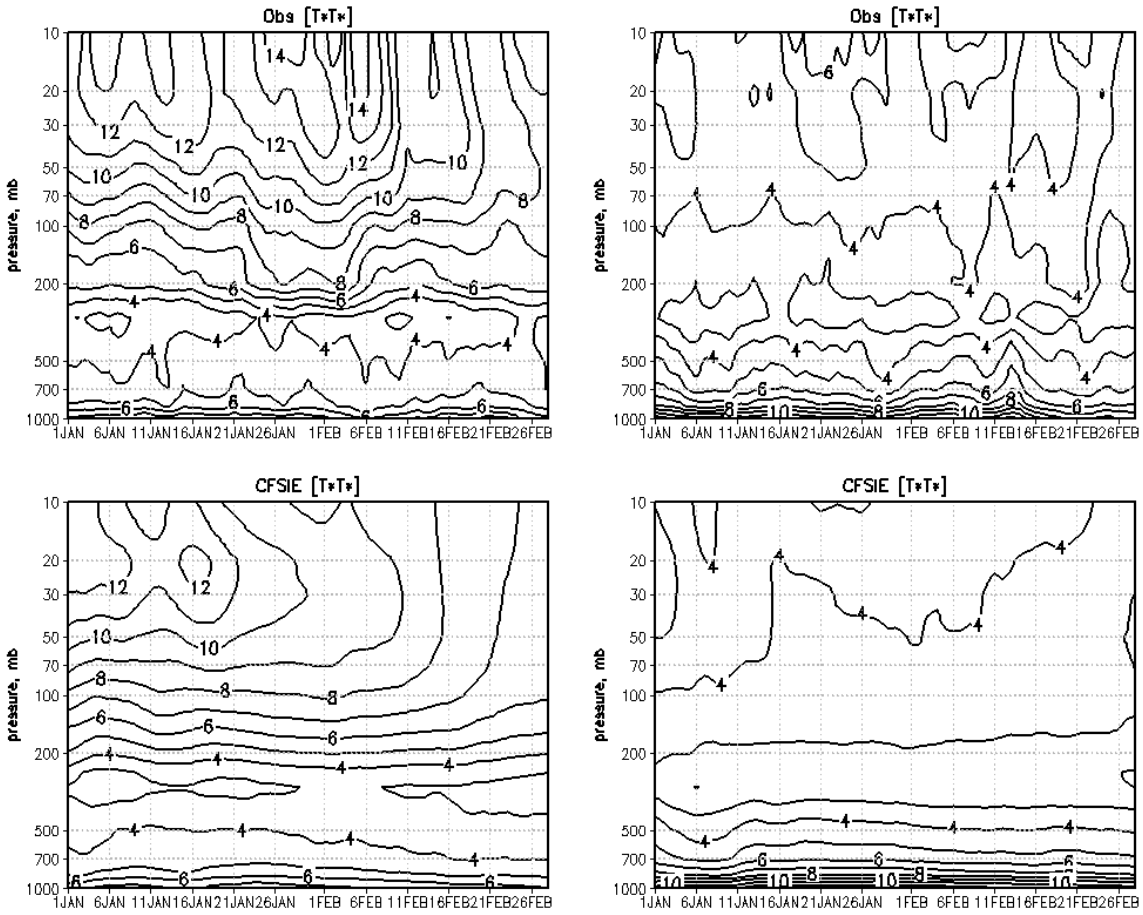

Figure 10 Vertical-time cross section of the temperature variance for wavenumer 1 (left) and 2 (right) from observations (top) and model simulations (bottom).

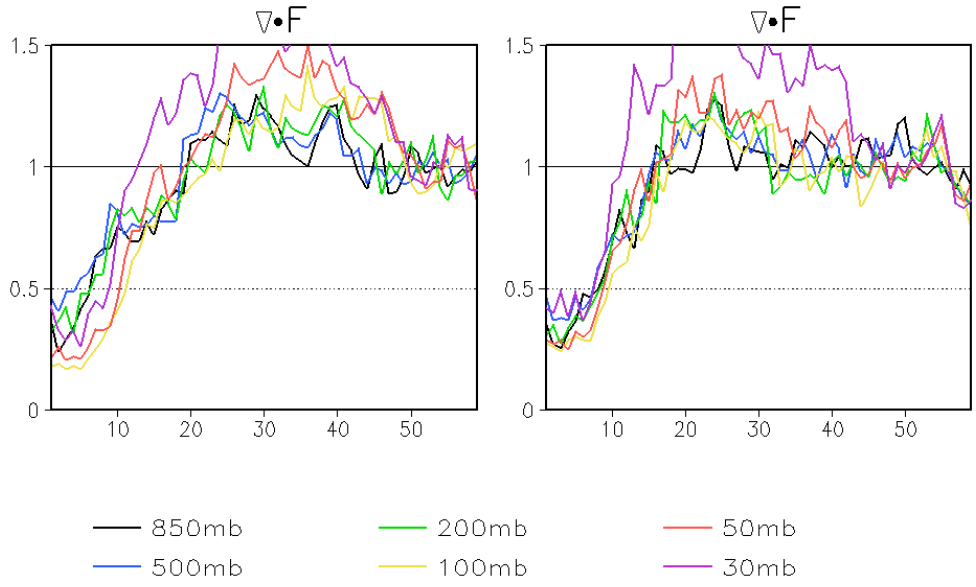

Figure 11 The squared error of EP flux divergence for wavenumbers 1 (left) and 2 (right).

Figure 11 shows the result for wavenumbers 1 and 2. The errors are also normalized by the saturation value, which is calculated as the last 10-day time average. The black curve corresponds to the 850 hPa level, the blue curve to the 500 hPa level, green to the 200 hPa level, yellow to the 100 hPa level, red to the 50 hPa level and purple to the 30 hPa level. The first feature of note is the large value of the initial error when compared to errors in the individual fields, and this is true for all levels. This result indicates that small errors in individual fields lead to large errors in the wave fluxes and their divergence. One might be tempted to say that this is an obvious result because the EP flux involves derivatives of second-order quantities. The second feature worth emphasizing is the systematic decrease in variability towards the end of boreal winter seen at upper levels. In the individual fields, this type of variation is characteristic mostly of the temperature field.

5. SUMMARY

The limit of predictability in the stratosphere versus troposphere in a coupled GCM was investigated using the National Center for Environmental Prediction (NCEP) Climate Forecast System (CFS). A set of identical twin experiments was obtained by using the interactive ensemble coupling strategy, where a single oceanic general circulation model (MOM3 of GFDL) was coupled to the ensemble average of multiple realizations (in this case 6) of an atmospheric GCM (NCEP Global Forecast System, GFS). The atmospheric GCMs are initialized from slightly different initial conditions, but the ocean state is the same. In this strategy, the atmospheric realizations represent different possible atmospheric states that have equally chances of occurrence.

We compared the normalized errors of zonal wind and temperature fields in the troposphere and stratosphere for various wave groups. The results show a large error growth in the stratosphere compared to troposphere.

We also investigated the predictability of sudden stratospheric warming events. The results suggest that the predictability of sudden stratospheric events is low because small errors in individual fields lead to large errors in the EP flux.

The connection between the behavior of the temperature and EP flux divergence is consistent with previous work, which emphasizes that the vertically propagation of planetary waves in the stratosphere depends on the permeability of the tropopause. The non-stationarity of the variability poses challenges for predictability theory, because it makes difficult to define the saturation value of the error growth. The last aspect we like to point out is the shorter limit of predictability in the stratosphere when compared to the troposphere. At lower levels, the limit of predictability is around 20 days, whereas at upper levels, the limit of predictability is reduced to about 10 days.

6. REFERENCES

Charlton, A. J. and L. M. Polvani, 2007: A new look at stratospheric sudden warming events: Part I. Climatology benchmarks. *J. Climate*, **20**, 449-469.

McIntyre, M. E., 1982: How well do we understand the dynamics of stratospheric warmings? *J. Meteor. Soc. Japan*, **60**, 37-65.

Stan, C. and B. P. Kirtman, 2007: The influence of atmospheric noise and uncertainty in ocean initial conditions on the limit of predictability in a coupled GCM, *J. Climate*, (submitted).